Factors influencing oil saturation and exploration fairways in the lower cretaceous Quantou Formation tight sandstones, Southern Songliao Basin, China

Kelai Xi[1], Yingchang Cao[1,2], Keyu Liu[1,2] and Rukai Zhu[3]

Abstract

Favorable exploration fairway prediction becomes crucial for efficient exploration and development of tight sandstone oil plays due to their relatively poor reservoir quality and strong heterogeneous oil saturation. In order to better understand the factors influencing oil saturation and favorable exploration fairway distribution, petrographic investigation, reservoir properties testing, X-ray diffraction analysis, oil saturation measurement, pressure-controlled mercury injection, and rate-controlled mercury injection were performed on a suite of tight reservoir from the fourth member of the Lower Cretaceous Quantou Formation (K_1q_4) in the southern Songliao Basin, China. The sandstone reservoirs are characterized by poor reservoir properties and low oil saturations. Reservoir properties between laboratory pressure conditions and in situ conditions are approximately the same, and oil saturations are not controlled by porosity and permeability obviously. Pores are mainly micro-scale, and throats are mainly nano-scale, forming micro- to nano-scale pore–throat system with effective connected pore–throat mainly less than 40%. Oil emplacement mainly occurs through the throats with average radius larger than 0.25 μm under original geological condition. Moreover, the samples with higher oil saturation show more

[1]School of Geosciences, China University of Petroleum (East China), Qingdao, China
[2]Laboratory for Marine Mineral Resources, Qingdao National Laboratory for Marine Science and Technology, Qingdao, China
[3]Research Institute of Petroleum Exploration & Development, Beijing, China

Corresponding authors.:
Kelai Xi and Yingchang Cao, No. 66, Changjiang West Road, Huangdao District, Qingdao, Shandong 266580, China.
Email: xikelai@upc.edu.cn; cyc8391680@163.com

scattered pore and throat distributions, but centered pore–throat radius ratio distribution. Pore–throat volume ratio about 2.3–3.0 is best for oil emplacement, forming high oil saturation. Quartz overgrowth, carbonate cements, and authigenic clays are the major diagenetic minerals. The reservoirs containing about 4–5% carbonate cements are most preferable for oil accumulation, and oil saturation increases with increasing of chlorite as well. The flow zone indicator is a reasonable parameter to predict favorable exploration targets in tight sandstone reservoirs. The reservoirs with flow zone indicator values larger than 0.05 can be regarded as favorable exploration targets in the K_1q_4 tight sandstones. According to the planar isoline of average flow zone indicator value, the favorable exploration targets mainly distribute in the delta plain distributary channel and deltaic front subaqueous distributary channel.

Introduction

As one of the most important unconventional hydrocarbon resources, tight sandstone oil have been paid more and more attention in recent years (Jia, 2017; Kang, 2016; Wang et al., 2015; Zou et al., 2013). Generally, tight sandstone reservoirs show large area of distribution and continuous or quasi-continuous oil accumulation (Pang et al., 2014; Zou et al., 2009). However, tight sandstone reservoirs are characterized by poor reservoir quality and significant heterogeneous oiliness due to the complicated diagenetic alterations modifying reservoir pore–throat structure and flow characteristics (Li et al., 2013; Wimmers and Koehrer, 2014; Zhou et al., 2016). As a result, tight sandstones commonly have oil shows, but resource abundance is low and oil distribution is significantly uneven (Li et al., 2013; Wei et al., 2016), suggesting that favorable exploration fairways prediction is quite essential in the efficient exploration and development of tight sandstone oil. Oil saturation is a typical parameter to reflect reservoir oiliness, which can be used to evaluate the tight sandstone reservoir potentials effectively (Law, 2002; Yang et al., 2013). Previous studies showed that porosity and permeability are no longer the critical factors for oil accumulation in tight sandstones (Lai et al., 2016; Xi et al., 2016; Zhu et al., 2013). Factors controlling oil saturation are complicated and various in tight sandstones, including pore–throat structure, diagenetic mineral wettability, pore water features, crude oil properties, and so on (Alotaibi et al., 2011; Buckley, 2001; Shanley and Cluff, 2015; Wardlaw, 1982; Zhao et al., 2015). Among them, pore–throat structure and reservoir seepage parameters are the most important ones (Wardlaw, 1982). Although some works have already paid attention to the influence of pore–throat structure and reservoir wettability on oil saturation (Qi et al., 2015; Wimmers and Koehrer, 2014; Xi et al., 2016), they are still not completely understood (Xi et al., 2016; Zeng et al., 2014). In addition, optimization parameter evaluation is a critical issue in favorable exploration targets prediction in tight sandstone reservoirs. Although oil saturation is very useful to evaluate the favorable exploration targets (Sun et al., 2015), it is not convenient to a large number of tests in most of studies due to tedious experiment processes and higher costs. Porosity and permeability are the most commonly

used and easily obtained parameters in sandstone reservoir studies. Therefore, it will be optimum if there is a parameter calculated from porosity and permeability can be used to predict the favorable exploration targets instead of oil saturation.

The objectives of this paper are primarily threefold: (1) investigate the reservoir property and oil saturation characteristics of the K_1q_4 tight sandstone reservoirs, (2) analyze the main factors influencing oil saturation in the K_1q_4 tight sandstone reservoirs, and (3) predict the favorable exploration fairways through optimization parameter evaluation in the K_1q_4 tight sandstone reservoirs.

Geological background

The Songliao Basin is a Jurassic–Neogene lacustrine basin in the north-eastern China (Figure 1), which is located between 42°25′ to 49°23′ N and 119°40′ to 128°24′ E with an area of about 26×10^4 km^2 (Zhang and Zhang, 2013). It can be further subdivided into seven first class tectonic zones (Zhou et al., 2012), namely the Western Slope Zone, Northern Pitching Zone, Central Depression Zone, Northeastern Uplift Zone, Southeastern Uplift Zone, Southwestern Uplift Zone, and Kailu Depression Zone (Figure 1). The study area, as
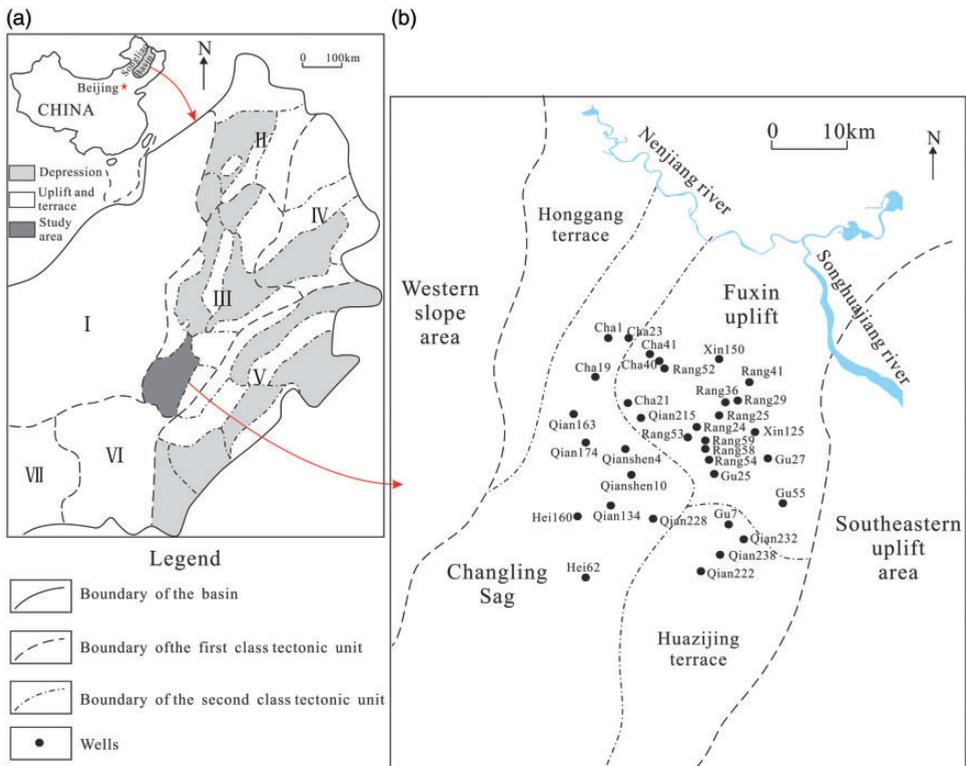

Figure 1. (a) Location map of the study area and subtectonic units of the Songliao Basin, (I) Western Slope Zone, (II) Northern Pitching Zone, (III) Central Depression Zone, (IV) Northeastern Uplift Zone, (V) Southeastern Uplift Zone, (VI) Southwestern Uplift Zone, (VII) Kailu Depression Zone and (b) the subtectonic units of the study area and well locations (from Xi et al. (2015)).

one of the most oil rich areas, belongs to the Central Depression Zone and consists of three secondary class tectonic units (Li et al., 2013), namely the Changling Sag, Huazijing Terrace, and Fuxin Uplift (Figure 1).

Based on the sediment infilling sequences and structures, the basin evolution can be divided into four phases: (1) a prerift phase, (2) a syn-rift phase, (3) a postrift phase, and finally (4) a compression phase (Zhang et al., 2009). Sediments that has filled the basin comprise the Lower Cretaceous Huoshiling (K_1h), Shahezi (K_1sh), Yingcheng (K_1yc), Doulouku (K_1d) and Quantou (K_1q) formations, the Upper Cretaceous Qingshankou (K_2qn), Yaojia (K_2y), Nenjiang (K_2n), Sifangtai (K_2s) and Mingshui (K_2m) formations, the Palaeogene Yian (Ny) formation, the Neogene Daan (Nd) and Kangtai (Nt) formations, and the Quaternary Pingyuan (Q) formation. Each formation can be further subdivided into different members (Figure 2). The studied section (Figure 2), that is the fourth member of Quantou Formation (K_1q_4), was deposited during the depression period of the tectonic evolution and mainly consists of deltaic sandstones and some interbedded mudstones (Li et al., 2013). According to oil analysis and source rock correlation, the first member of the Qingshankou Formation (K_2qn_1), which just overlies K_1q_4, is the main source rock of K_1q_4 reservoirs (Li et al., 2013; Zou et al., 2005). Oil generation ($Ro = 0.5\%$) in the K_2qn_1 began at a depth of about 1350–1450 m and at a temperature of 80–85°C (Dong et al., 2014). The K_2qn_1 commonly developed over pressure, whereas the K_1q_4 sandstone reservoir showed normal pressure at most of the studied intervals. Thus, oil can migrate from source rocks to reservoirs easily, drove by the differential pressure (Xi et al., 2015).

Databases and methods

Reservoir porosity and permeability with corresponding oil saturation of 8529 data points, six porosity and permeability data under over burden pressure, well test and production test data of several wells, 237 pressure-controlled mercury injection (PMI) testing data, and nine rate-controlled mercury injection (RMI) testing data were collected from Research Institute of Petroleum Exploration & Development of the Jilin Oilfield Company, PetroChina.

Over 300 polished thin sections and about 210 blue or red epoxy resin-impregnated thin sections were prepared for the analysis of reservoir petrology, diagenesis, visual pore, and oil micro-occurrence characteristics. Thin sections were partly stained with Alizarin Red S and K-ferricyanide for carbonate mineral identification. A total of 105 reservoir sandstone samples were analyzed for whole-rock (bulk) and clay fraction (<2 μm) mineralogy using XRD. Preparation, analyses, and interpretation procedures were modified from Hillier (2003) and Moore and Reynolds (1997). About 5.0 g of each sample was crushed, milled in ethanol in a McCrone micronizing mill, and then dried at 60°C. Randomly oriented powders were prepared by top loading into polymethylmethacrylate sample holders designed with concentric circular geometry grooved shallow wells. The powder diffraction patterns were the collected using a D/MAX, 2500 X-ray diffractometer with Cu Kα radiation. All XRD data were first analyzed for phase identification with the search-match module of the EVA software using the reference databases ICDD PDF-2 and COD. After phases were identified, they were further analyzed based on the Rietveld quantitative X-ray diffraction refinement approach.

Except for the 237 PMI testing data from the Jilin oil field, 52 cylindrical samples of 2.54 cm in diameter and about 4 cm in length were measured using an AutoPore IV9505 mercury porosimeter following the standard SY/T 5346–2005 of China. Maximum intrusion
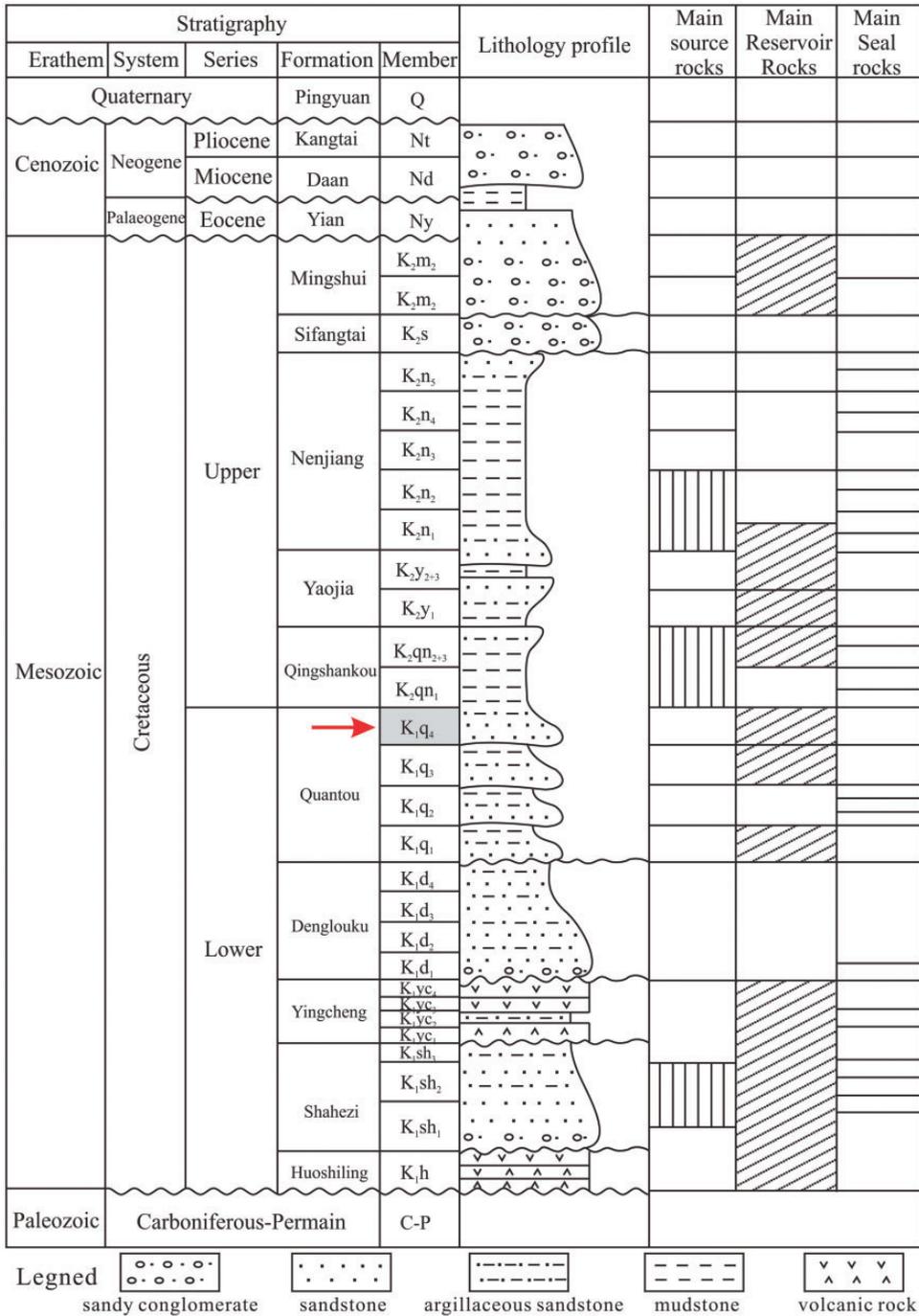
Stratigraphy					Lithology profile	Main source rocks	Main Reservoir Rocks	Main Seal rocks
Erathem	System	Series	Formation	Member				
Cenozoic	Quaternary		Pingyuan	Q				
	Neogene	Pliocene	Kangtai	Nt				
		Miocene	Daan	Nd				
	Palaeogene	Eocene	Yian	Ny				
Mesozoic	Cretaceous	Upper	Mingshui	K_2m_2				
				K_2m_1				
			Sifangtai	K_2s				
			Nenjiang	K_2n_5				
				K_2n_4				
				K_2n_3				
				K_2n_2				
				K_2n_1				
			Yaojia	K_2y_{2+3}				
				K_2y_1				
			Qingshankou	K_2qn_{2+3}				
				K_2qn_1				
		Lower	Quantou	K_1q_4				
				K_1q_3				
				K_1q_2				
				K_1q_1				
			Denglouku	K_1d_4				
				K_1d_3				
				K_1d_2				
				K_1d_1				
			Yingcheng	K_1yc_4				
				K_1yc_3				
				K_1yc_2				
				K_1yc_1				
			Shahezi	K_1sh_3				
				K_1sh_2				
				K_1sh_1				
			Huoshiling	K_1h				
Paleozoic	Carboniferous-Permain			C-P				

Legned

sandy conglomerate   sandstone   argillaceous sandstone   mudstone   volcanic rock

Figure 2. Generalized Mesozoic–Quaternary stratigraphy of the Songliao Basin, showing major oil and gas combinations (from Xi et al. (2015)).

pressure was 101.32 MPa, corresponding to a pore–throat size of approximately 1.0 nm. After reaching the highest pressure, the pressure was then gradually decreased and the mercury extruded from the samples. Thus, intrusion and extrusion curves as well as various characterization parameters were obtained, such as average pore–throat size, mercury intrusion saturation, residual mercury saturation, displacement pressure, medium saturation pressure, and so on.

Except for the nine RMI testing data from the Jilin Oilfield, six cylindrical samples with 2.54 cm in diameter and about 4 cm in length were measured on an ASPE-730 rate-controlled mercury porosimeter following the standard Q/SY DQ1526–2012 of the Daqing Oilfield, PetroChina. This method, based on pressure fluctuations, can be used to identify and classify the pores and throats in sandstones and may provide much more information compared to PMI testing. In the RMI experimental method, mercury is injected into the reservoirs at an extremely low constant rate and the mercury pressure and volume are accurately measured (Zhao et al., 2015). Mercury injection rate was done at a quasi-static constant value of 5×10^{-5} ml min^{-1}, and a maximum intrusion pressure of 6.2 MPa, corresponding to a pore–throat size of 0.12 μm. Using this method, mercury intrusion curves of the pore, throat, and total were obtained, respectively, as well as various characterization parameters, such as pore radius, throat radius, and pore–throat radius ratio.

Among all the analysis methods used in this study, the petrographic observations were done in the Key Laboratory of Basin Analysis and Reservoir Geology of China University of Petroleum. XRD analyses were done in the Key Laboratory of Oil and Gas Reservoir of PetroChina. PMI and RMI were done in the Research Institute of Petroleum Exploration & Development of Daqing Oilfield, PetroChina.

Results

Reservoir properties and oil saturation

Reservoir properties. Under ambient laboratory pressure, porosities of core samples in the K_1q_4 sandstone range from 1.7 to 20% (mainly 4.0–14%) with an average of 8.54% (Figure 3(a)), while the horizontal permeability ranges from 0.01 to 44.5 mD (mainly <1.0 mD) with an average of 0.493 mD (Figure 3(b)), showing quite poor reservoir properties overall. In order to investigate the influence of overburden pressure on porosity and permeability, several core samples were measured under different overburden pressures. It shows that porosity and permeability decreased slightly with increasing overburden pressure (Figure 3(c) and (d)). In contrast, the reduction of porosity and permeability mainly happened in the stage of overburden pressure less than 10 MPa (Figure 3(c) and (d)). Afterward, it shows insignificant trends between overburden pressure and porosity as well as permeability (Figure 3(c) and (d)). Compared to the reservoir properties measured under ambient laboratory pressure, porosity reduction was less than 0.5% only in most of the samples when overburden pressure was increased to about 30 MPa (Figure 3(c)). Moreover, the permeability under 30 MPa confining pressure is within the same order of magnitude as under ambient laboratory pressure (Figure 3(d)). This means that the reservoir properties measured from ambient laboratory pressure are not much different from those measured under overburden pressure conditions, indicating that reservoir rocks are lack of fractures and do not expand after being removed from the wells. Thus, porosity and permeability
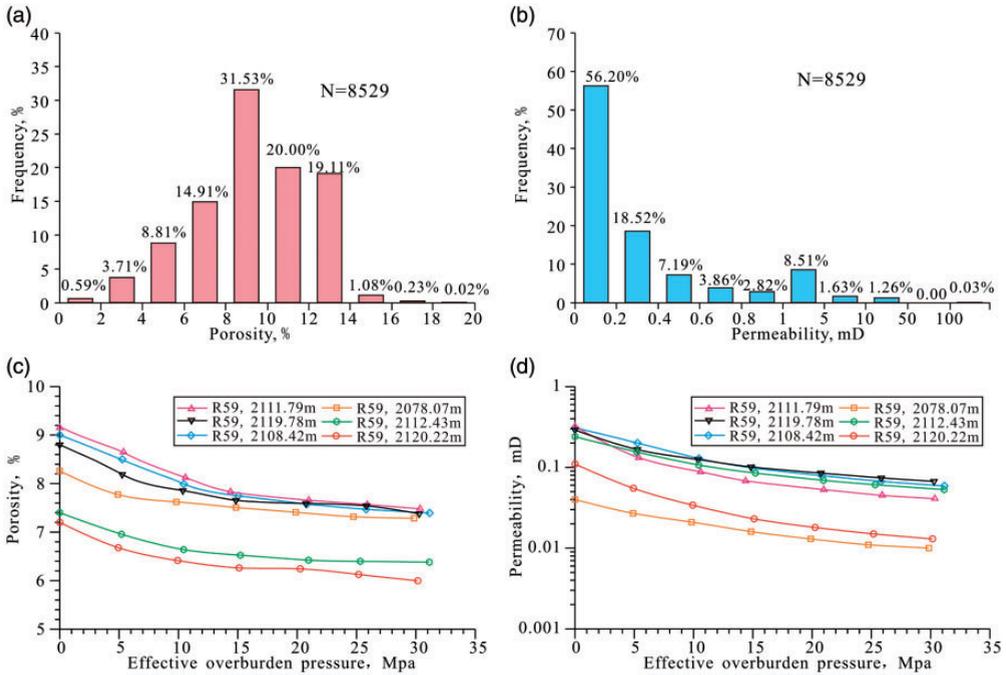
Figure 3. Porosity and permeability characteristics under laboratory pressure (a, b) and overburden pressure (c, d) conditions.

measured under ambient laboratory pressure can be used to approximately evaluate reservoir quality.

Oil saturation characteristics. Oil saturation in the K_1q_4 tight sandstone reservoirs is relatively low, ranging from 0.1 to 73.2% with an average of 23.5% (Figure 4(a)). More than 40% of the reservoirs have oil saturation less than 20% (Figure 4). Distribution of oil saturation is quite scattered, indicating quite heterogeneous oiliness in the studied reservoirs (Figure 4(a)). Moreover, there is no apparent relationship between oil saturation and reservoir properties. Reservoirs with similar porosity and permeability values can show significantly different oil saturations (Figure 4(b)).

Pore and throat characteristics

According to RMI, pore radius in the K_1q_4 tight sandstone reservoirs ranges from 128.97 to 152.31 μm with an average of 143.85 μm (Figure 5), while pore–throat radius varies between 0.197 and 0.869 μm with a mean value of 0.389 μm (Figure 5). As a whole, pores in the K_1q_4 tight sandstone reservoirs are mainly of micro-scale, whereas pore–throats are mainly of nano-scale, forming micro- to nano-scale pore–throat system.

Pore connectivity is a key factor influencing reservoir infiltration capacity. In the bi-logarithm graph of PMI, the curve peak (point B) represents the ending position of connected pore–throats for mercury intrusion, which means that pore connectivity becomes poorer progressively after this point (Yu et al., 2015). The curve peak (point B) in the
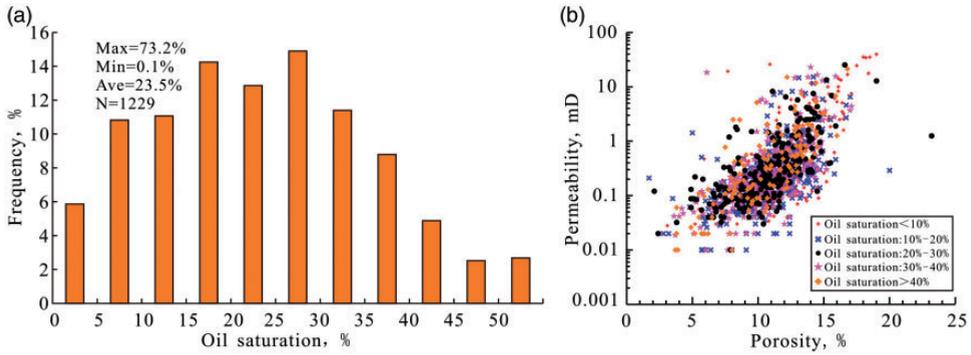
Figure 4. Oil saturation distribution and relationship between reservoir properties and oil saturation in the K_1q_4 tight sandstones.
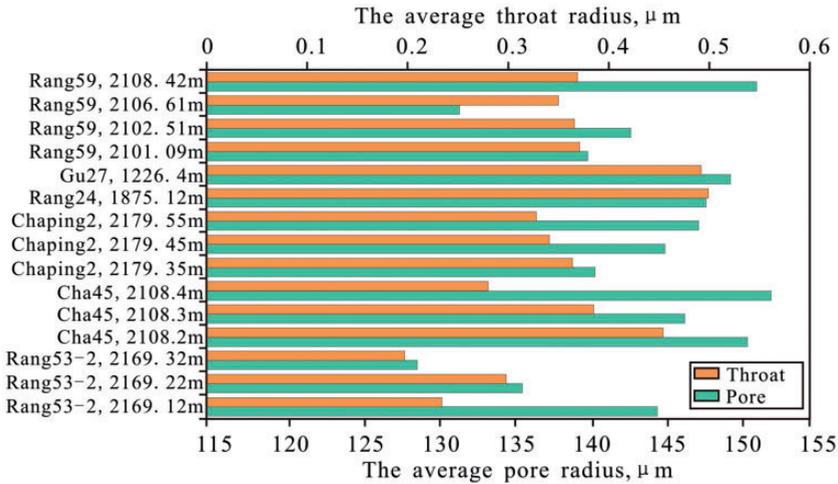

Figure 5. Pore and throat size in the K_1q_4 tight sandstone reservoirs.

bi-logarithm graph has a corresponding point (point C) in the normal mercury injection curve (Figure 6). If we define the displacement pressure in the mercury injection curve as point A, the pores and throats between point A and C can be regarded as effective connected pore–throat system (Figure 6). In the K_1q_4 tight sandstone reservoirs, most of the samples are characterized by poor pore connectivity with effective connected pore–throat system mainly less than 40% (Figure 6). There is a negative relationship between the ratio of connected pore–throats and reservoir permeability. However, the reservoir porosity and the ratio of connected pore–throats do not appear to have any significant correlation (Figure 6).

Diagenetic minerals

Several diagenetic minerals are present in the K_1q_4 tight sandstone reservoirs with quartz overgrowth, carbonate cements, and clay minerals being the major cementing
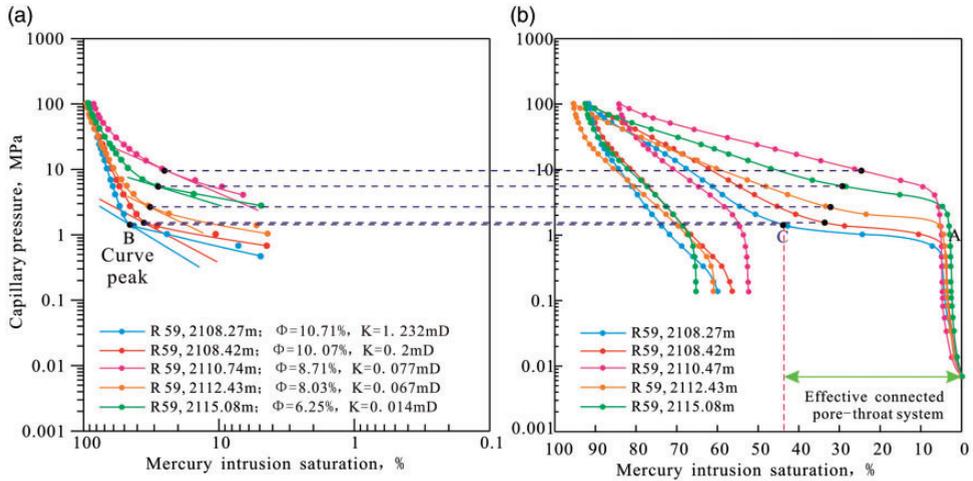
Figure 6. (a) Bi-logarithm graph and (b) normal mercury injection curve of PMI.
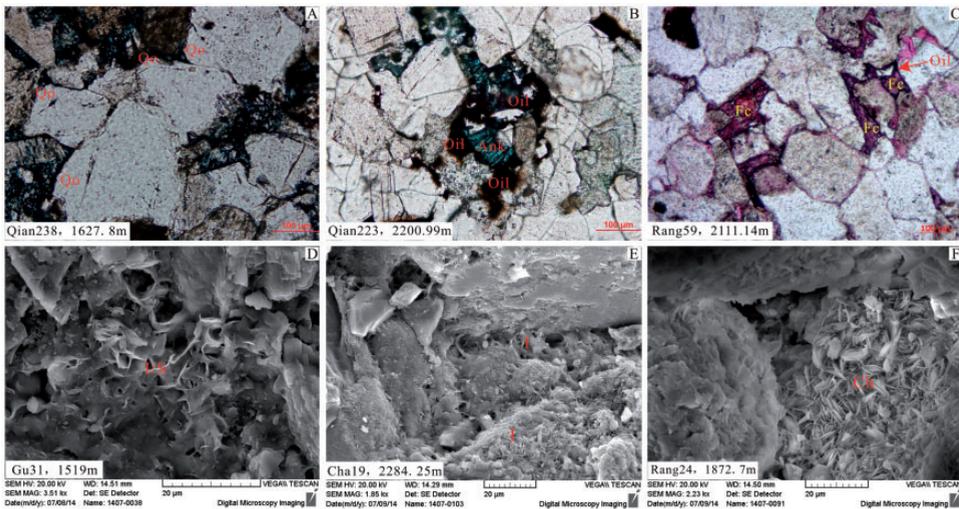

Figure 7. Characteristics of diagenetic minerals in the K_1q_4 tight sandstone reservoirs: (a) Photomicrographs of thin section showing characteristics of quartz overgrowth, (b) photomicrographs of thin section showing characteristics of ankerite and oil accumulation, (c) photomicrographs of thin section showing characteristics of ferrocalcite and oil accumulation, (d) photomicrographs of SEM showing characteristics of mixed-layer I/S, (e) photomicrographs of SEM showing characteristics of illite, and (f) photomicrographs of SEM showing characteristics of chlorite. Ank: ankerite; Ch: chlorite; Fc: ferrocalcite; I: illite; I/S: mixed-layer I/S; Qo: quartz overgrowth.

agents (Figure 7). They had significant impact on reservoir properties and probably had significant effects on oil saturation as well. Authigenic quartz, mainly showing as partial to complete syntaxial overgrowths, is one of the most common cements in the K_1q_4 tight sandstone reservoirs. Quartz overgrowth occurs as relatively large aggregates of microcrystalline or macrocrystalline with approximately 30–100 μm in size (Figure 7(a)).

Table 1. Content of clay minerals measured by XRD and related oil saturation.

Well	Depth (m)	I/S (%)	I (%)	C (%)	Oil saturation (%)
R59	2099.77	59	15	26	19.5
R59	2100.54	71	14	15	18.2
R59	2100.94	56	13	31	18.6
R59	2101.76	54	12	34	25.6
R59	2102.98	47	10	43	18.3
R59	2108.11	35	9	56	38.1
R59	2109.91	42	14	44	25.7
R59	2111.79	51	7	42	33.5
R59	2112.42	38	10	52	36.1
R59	2112.6	44	7	49	25.1
R59	2116.34	44	10	46	31.8
R59	2117.81	33	10	57	32.1
R59	2120.59	60	14	26	14.2

I/S: illite/smectite; XRD: X-ray diffraction.

Carbonate cements, mainly including ferrocalcite and ankerite, occur as scattered euhedral rhombs, and pore-filling blocky or mosaic aggregates (Figure 7(b) and (c)). Interestingly, oil preferred to accumulate in the residual pore spaces around carbonate cements (Figure 7(b) and (c)). The most common authigenic clay minerals are mixed-layer illite/smectite (I/S), illite and chlorite. Honeycomb-textured I/S with $R = 1$ or $R = 3$ acts as the dominating authigenic clay minerals in primary pores and on grain surfaces (Figure 7(d) and Table 1). Fibrous and flaky illite mainly presents in primary pores and sometimes on grain surfaces or in feldspar dissolution pores, locally bridging pore–throats (Figure 7(e)). Chlorite appears as scattered flakes in the studied reservoirs, showing variabilities in different pore spaces (Figure 7(f)).

Discussions

Factors influencing oil saturation

Pore–throat parameters

  Pore–throat size and distribution. Pore–throat sizes of the K_1q_4 tight sandstone reservoirs distribute over a large range. According to mercury injection data, about 2.0–5.0% of the throats have average radius less than 0.01 μm, 25–40% of the throats have average radius ranging from 0.01 to 0.1 μm, 10–30% of the throats have average radius varying from 0.1 to 0.25 μm, and 15–50% of the throats have average radius ranging from 0.25 to 1.0 μm (Figure 8). Oil saturation appears to have been significantly impacted by the pore–throat sizes, especially the range of pore–throats with average radius from 0.25 to 1.0 μm (Figure 8). Oil saturation is shown to be positively correlated with the percentages of 0.25–1.0 μm pore–throat size, which primarily corresponds to oil saturation ranges of >30% (Figure 8(a)). For the pore–throats with average radius of <0.25 μm, there appears no correlation between oil saturation and the percentage of the pore–throats (Figure 8(b) and (c)), which suggests that oil emplacement mainly occurred through the pore–throats with average radius greater than 0.25 μm in the studied reservoirs. This is because the
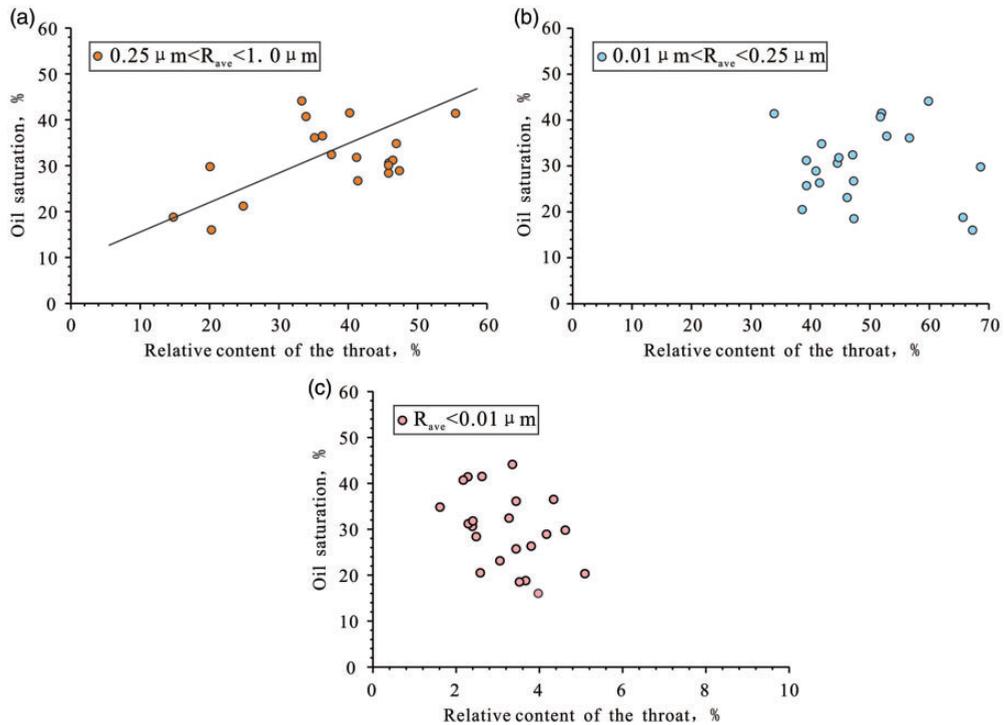
Figure 8. Relationship between relative content of the throat and oil saturation in different throat size ranges.

studied reservoirs are mainly water-wet with contact angle ranging from 22.83° to 38.32° (38 samples in total) and capillary entry pressures for the oil emplacement increase with decreasing pore–throat radius in a water-wet system generally. In order to displace the oil into the water-wet reservoirs in this area, about 300 m oil column height is needed to provide the capillary entry pressure. In the studied area, however, the oil column height is not enough. Hence, the pore–throats with average radius smaller than 0.25 μm are probably too small for the oil to enter into the water-wet reservoirs under the original geological conditions of this area (Xi et al., 2016).

The ranges of pore radius, pore–throat radius, and pore–throat radius ratio are different in the samples with different oil saturations. Generally, oil saturation increases with increasing average pore and throat radius. Samples with higher oil saturation show more scattered pore and throat distributions, but more centered pore–throat radius ratio distribution (Figure 9). For samples with oil saturation higher than 30%, pore and pore–throat radius distributes in relative large ranges with most of the throat radii being larger than 0.5 μm, while the pore–throat radius ratios are within relative narrow ranges from about 100 to 300 (Figure 9(a)). In contrast, samples with oil saturation lower than 30%, the pore and pore–throat radius distributes in narrow ranges with throat radius rarely exceeding 0.5 μm, while the corresponding pore–throat radius ratio distributes over relatively large ranges from about 200 to 800 (Figure 9(b) and (c)). This suggests that pore–throat sizes and their distribution are particularly significant factors controlling oil saturation in tight sandstone
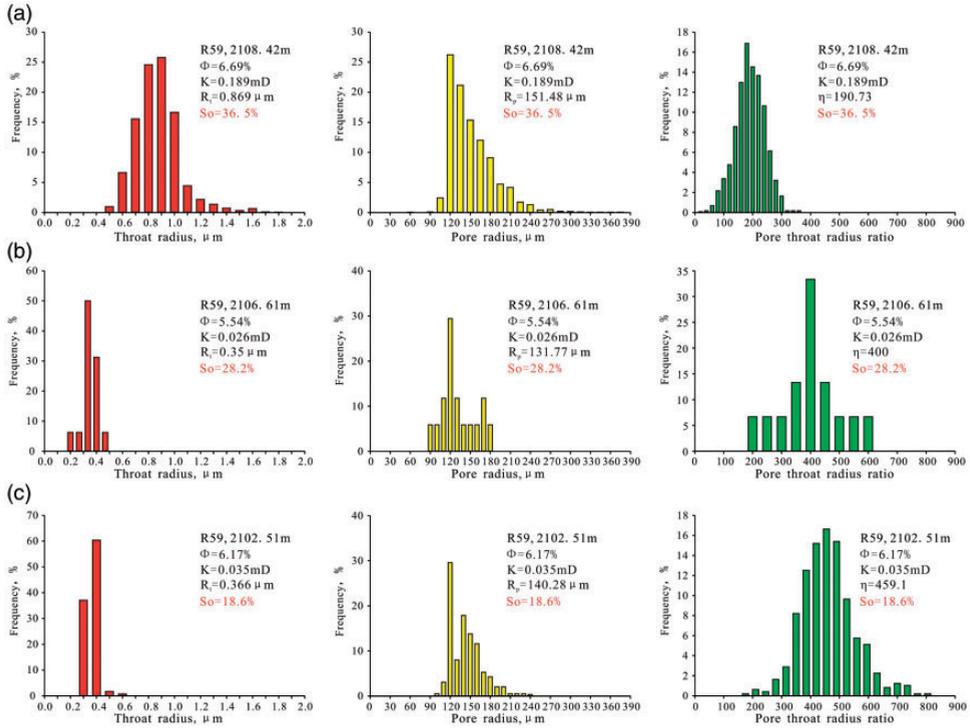
Figure 9. Distributions of pore–throat radius, pore radius, and pore–throat radius ratio in the samples with different oil saturation. R_t: throat radius; R_p: pore radius; η: pore–throat radius ratio.

reservoirs. As tight sandstone reservoirs are mainly dominated by small pore–throat size, larger pores and pore–throats, which are favorable for oil emplacement, would exist in the reservoirs when pore and pore–throat distributions are scattered. Sorting coefficient of pore–throat measured by the PMI can reflect the concentration and dispersion degree of pores and pore–throats in sandstone reservoirs. Quantitative statistics show that (1) oil saturations are generally greater than 20% in reservoirs with pore–throat sorting coefficients of >2.6; (2) oil saturations are mainly greater than 30% when the pore–throat sorting coefficients are >3.0. This further suggests that the small percentage of large pore–throats in the reservoirs has significant contributions to oil emplacement in tight sandstone reservoirs.

Pore–throat volume ratio. In samples with different permeabilities and pore–throat size distributions, the total mercury saturation is contributed by different ratio of pore mercury saturation and throat mercury saturation. RMI suggests that the contributions from pore–throats to the total mercury saturation increase with decreasing permeability, while the contributions from pores to the total mercury saturation increase with increasing permeability (Figure 10(a) to (c)). Combined with oil saturation measurements, the total mercury saturation curve can be viewed as a function of pore–throat radius, exhibiting a quite consistent pore mercury saturation curve when oil saturation is higher than 30% (Figure 10(a)). On the contrary, the total mercury saturation curve accords well with the pore–throat
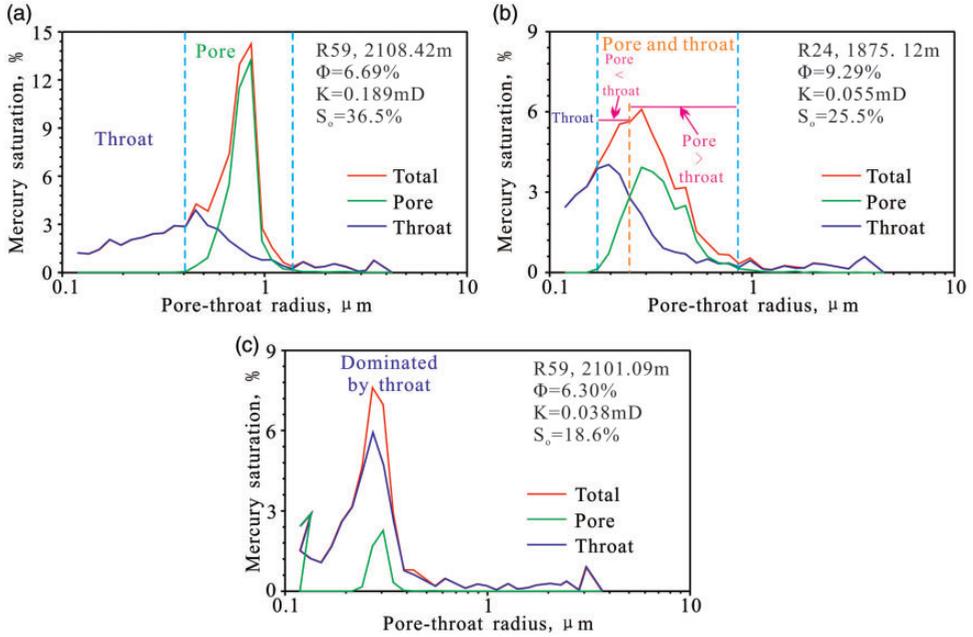
Figure 10. Characteristics of pore and throat contributions to total mercury saturation in the samples with different oil saturation.

mercury saturation curve when oil saturation is less than 20% (Figure 10(c)). For samples with oil saturation ranging from 20 to 30%, the total mercury saturation is contributed both by pores and pore–throats (Figure 10(b)). The contribution from pores is more significant to the total mercury saturation over that from pore–throats at the early stage of mercury injection (Figure 10(b)). With increasing displacement pressure and decreasing pore–throat radius for mercury intrusion, the contribution from pores to the total mercury saturation decreases while that from the pore–throats increases (Figure 10(b)). After a certain pore–throat radius, the contribution from the pore–throats would become more significant over that from pores. For example, the sample with 25.5% oil saturation shows that the contribution from the pore–throats to the total mercury saturation is much more significant than that from the pores when the pore–throat radius is smaller than 0.25 μm (Figure 10(b)). Therefore, tight sandstones with total reservoir spaces dominated by pores are more favorable for oil accumulation. Oil saturation decreases gradually with increasing contributions from pore–throats to the total reservoir space volumes.

In the PMI curve, mercury intrusion saturation represents the total volume of pores and pore–throats, while the mercury extrusion saturation represents the pore–throat volume and the residual mercury saturation represents the pore volume in the sandstone reservoirs, respectively. Hence, the pore–throat volume ratio can be calculated by equation (1) (Yu et al., 2015)

$$V_r = S_r/(S_{max} - S_r) \qquad (1)$$

where V_r is average pore–throat volume ratio, S_r is residual mercury saturation, and S_{max} is maximum mercury intrusion saturation, %.

According to the calculated results of pore–throat volume ratios and the corresponding oil saturation (Table 2), there appears to be a nonmonotonic correlation between oil saturation and pore–throat volume ratio in the K_1q_4 tight sandstone reservoirs. Oil saturation of the reservoir increases initially and then falls with increasing pore–throat volume ratio (Figure 11). Overall, oil saturation increases with increasing pore–throat volume ratio when the pore–throat volume ratio is less than 2.5–3.0 (Figure 11). Oil saturation decreases with increasing pore–throat volume ratio when it is larger than 2.5–3.0 (Figure 11). Further analyses demonstrate that oil saturations of reservoir are generally less than 30% when the pore volume ratio is less than 1.7 and ranges from 10 to 40% when pore–throat volume ratio is about 1.7–2.3 (Figure 11). When the pore volume ratio reaches 2.3–3.0, the oil saturations in the reservoir are primarily over 30% with some samples even exceeding 50% (Figure 11). However, oil saturations would begin to decrease when the pore volume ratio is over 3.0, corresponding to an oil saturation of less than 40% (Figure 11). Consequently, pore–throat volume ratio about 2.3–3.0 is best for oil emplacement in the K_1q_4 tight sandstone reservoirs, forming high oil saturation. This is because the total reservoir space volume is mainly contributed by pore–throats when the pore–throat volume ratio is too small. In this condition, the reservoir capability is limited and not favorable for oil accumulation. On the contrary, the total reservoir space volume is mainly contributed by pores when the pore–throat volume ratio is large. In this scenario, the reservoirs are lack of effective pore–throats and thus the connectivity is poor, impeding oil accumulation.

Diagenetic minerals influence on oil saturation

Carbonate cements. Different with the relationship between the content of carbonate cements and porosity in sandstone reservoirs, the relationship between carbonate cement content and oil saturation shows a nonmonotonic correlation in the K_1q_4 tight sandstone reservoirs (Figure 12 and Table 3). When the carbonate cement content is lower than 4–5%, oil saturation is positively correlated with the carbonate cement content (Figure 12). When the carbonate cement content is higher than 5%, oil saturation begins to decrease with increasing carbonate cement content (Figure 12). The highest oil saturation corresponds to the carbonate cement content of 4–5% in the K_1q_4 tight sandstone reservoirs (Figure 12). This suggests that there are probably very limited pore spaces preserved for oil accumulation if the carbonate cement content is greater than 5% due to cementation. When carbonate cements are less than 5%, more and more residual pore spaces around the cements can turn into oil-wet with increasing carbonate cements (Buckley, 2001), promoting oil emplacement and accumulation. Furthermore, the crude oil was mainly free oil characterized by low content of resins and asphaltenes, ranging from 9.8 to 19.5% with an average of 14.84% in the studied tight sandstone reservoirs. This type of crude oil flows easily due to small adhesion. Petrological evidence showed that oil turns to preferentially accumulate in the carbonate cementation residual pore spaces (Figure 7(b) and (c)). This further supports the favorable impacts of oil-wet carbonate cements on oil accumulation in the K_1q_4 sandstone reservoirs.

Clay minerals. Mixed-layer I/S, illite, and chlorite are the major authigenic minerals influencing reservoir properties in the K_1q_4 tight sandstone. They can impact oil emplacement and accumulation significantly. Oil saturation decreases with increasing I/S and illite contents, indicating a negative influence on oil accumulation (Figure 13(a) and (b)), while oil

Table 2. Results of pressure-controlled mercury injection and related oil saturation.

Well	Depth (m)	S_{max} (%)	S_r (%)	V_r	Oil saturation (%)
G21	1156.10	81.69	47.23	1.37	14.00
G26	1261.77	85.06	51.87	1.56	11.60
G26	1263.90	86.14	52.81	1.58	25.00
G22	1272.34	78.85	44.69	1.31	27.90
G31	1514.96	81.86	53.04	1.84	31.00
G36	1515.72	81.21	58.99	2.66	49.10
G36	1518.01	94.32	66.55	2.40	35.10
G7	1551.84	84.16	57.23	2.13	23.20
G7	1556.43	70.29	44.56	1.73	30.60
G11	1558.58	73.49	45.75	1.65	26.60
G14	1565.46	87.85	58.13	1.96	20.30
G17	1584.86	88.52	57.32	1.84	12.50
G24	1624.16	81.71	52.71	1.82	30.90
G19	1651.51	89.23	68.97	3.41	38.40
G13	1702.85	80.28	59.04	2.78	50.70
G13	1716.87	74.76	56.81	3.17	36.40
Q162-2	2068.92	94.91	68.73	2.63	51.70
R59	2105.92	92.18	59.17	1.79	28.40
R59	2106.27	92.33	58.51	1.73	18.80
R59	2106.47	91.83	56.59	1.61	23.10
R59	2107.39	91.93	59.06	1.80	18.50
R59	2108.42	91.80	56.43	1.60	26.30
R59	2109.92	93.59	61.92	1.95	25.70
R59	2110.22	84.13	52.30	1.64	20.30
R59	2110.35	93.76	63.75	2.12	20.50
R59	2110.74	91.87	61.68	2.04	26.70
R59	2111.48	92.46	62.62	2.10	28.90
R59	2111.79	92.76	61.41	1.96	30.60
R59	2112.43	95.24	60.89	1.77	36.10
R59	2114.92	88.02	59.40	2.08	31.20
R59	2115.08	92.58	65.39	2.40	32.00
R59	2115.67	88.39	60.82	2.21	31.80
R59	2117.27	94.76	62.60	1.95	41.50
R59	2117.72	93.22	64.16	2.21	29.80
R59	2118.09	87.87	56.40	1.79	32.40
R59	2119.78	90.40	61.18	2.09	34.80
R59	2119.99	87.85	58.14	1.96	40.70
R59	2120.23	92.09	64.09	2.29	21.00
R59	2120.85	90.15	51.58	1.34	21.20
R59	2121.29	96.40	62.85	1.87	30.10
R59	2121.62	87.99	59.98	2.14	24.30
R59	2125.72	91.49	59.62	1.87	16.00
R59	2128.18	92.82	58.17	1.68	19.20
R59	2128.50	96.08	61.89	1.81	20.50
C28	2138.73	75.09	57.14	3.18	28.90
C26	2275.46	78.80	54.00	2.18	26.20

Note: V_r is average pore–throat volume ratio, S_r is residual mercury saturation, S_{max} is maximum mercury intrusion saturation, %.
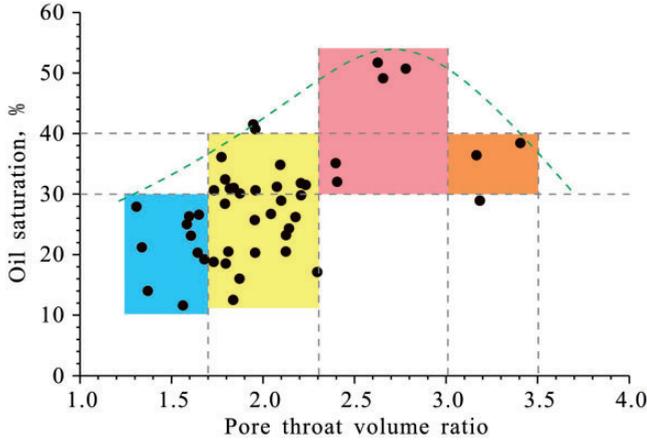
Figure 11. Relationship between pore–throat volume ratio and oil saturation in the K₁q₄ tight sandstones.
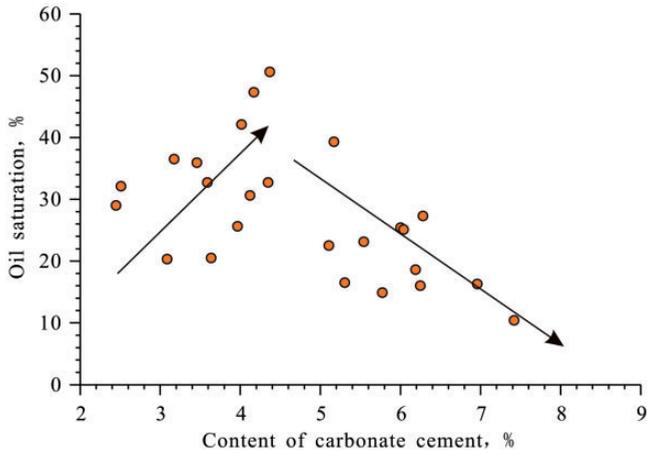

Figure 12. Relationship between content of carbonate minerals and oil saturation in the K₁q₄ tight sandstone reservoirs.

saturation increases with increasing chlorite content, showing a positive influence on oil accumulation (Figure 13(c)). This is probably because that mixed-layer I/S and illite, which are water-wet, block the pore–throats of the reservoirs. Although plate-like chlorite can, as illite and I/S, reduce the porosity and permeability, it is oil-wet and has an affinity with oil and can thus promote oil emplacement and accumulation through spontaneous imbibition of oil within tight sandstone reservoirs (Buckley, 2001; Xi et al., 2015).

Oil saturation for the favorable exploration fairway

Oil saturation is one of the most important parameters for determining favorable exploration target in tight sandstone reservoirs. According to well testing and production testing

Table 3. Content of carbonate cement and related oil saturation.

Well	Depth (m)	Porosity (%)	Permeability (%)	Carbonate (%)	Oil saturation (%)
C45	2107.745	10	0.22	5.54	23.1
Q221	2112.3	10.9	0.101	4.35	32.7
Q223	2187.14	6.2	0.057	6.96	16.3
Q223	2205.7	7.9	0.12	5.31	16.5
Q223	2216.69	9.4	0.114	3.17	36.5
Q223	2217.33	8	0.188	6.28	27.3
Q223	2223.81	8	0.086	5.10	22.5
Q223	2191.23	4.7	0.046	3.08	20.3
Q228	2338	9.9	n	4.01	42.1
Q228	2338.61	12.6	0.28	4.17	47.3
Q228	2338.72	12.9	0.33	4.37	50.6
Q228	2339.1	8.9	0.19	5.17	39.3
Q228	2339.43	10.6	0.33	3.46	35.9
Q228	2340.84	8.1	0.21	1.97	25.1
R53	2109.4	6.4	0.08	2.45	29
R58	2036.1	9.2	n	4.12	30.6
R58	2037.8	10.6	n	3.59	32.7
R58	2042.17	11.6	0.663	5.77	14.9
R58	2042.7	9.5	0.127	6.19	18.6
R59	2099.975	7.1	0.08	3.96	25.6
R59	2101.76	8	0.16	6.00	25.4
R59	2103.215	7.8	0.17	6.04	25.1
R59	2110.08	10	0.33	2.51	32.1
R59	2112.605	8.2	0.24	6.25	16
R59	2117.915	12.4	0.48	3.63	20.5
R59	2125.72	8.7	0.09	7.42	10.4

n: no data.

data, the tight sandstones are mainly oil reservoirs and oil–water reservoirs, but without water reservoirs or dry layers, when the oil saturations are larger than 30% (Figure 14(a) and (b)). For reservoir units with oil saturations between 20 and 30%, the tight sandstones are mainly oil–water reservoirs with some water reservoirs, but without dry layers (Figure 14 (a) and (b)). However, the tight sandstones are mainly water reservoirs and dry layers, but without oil reservoirs and oil–water reservoirs, when the oil saturations are lower than 20% (Figure 14(a) and (b)). Accordingly, the lowest oil saturation for the favorable exploration targets can be set as 20% in the K_1q_4 tight sandstone reservoirs, and the reservoirs with oil saturation greater than 30% may provide relative high oil production.

Parameters for exploration fairway prediction

Although oil saturation is quite useful in evaluating favorable exploration targets, it is not always convenient to conduct a large number of tests in most cases owing to its tedious experimental procedure and higher costs. Generally, porosity and permeability are the most commonly used and easily obtained parameters in sandstone reservoir studies. However, porosity and permeability are not the main controlling factors for oil saturation in tight sandstone reservoirs due to the complicated pore–throat structures (Xi et al., 2016;
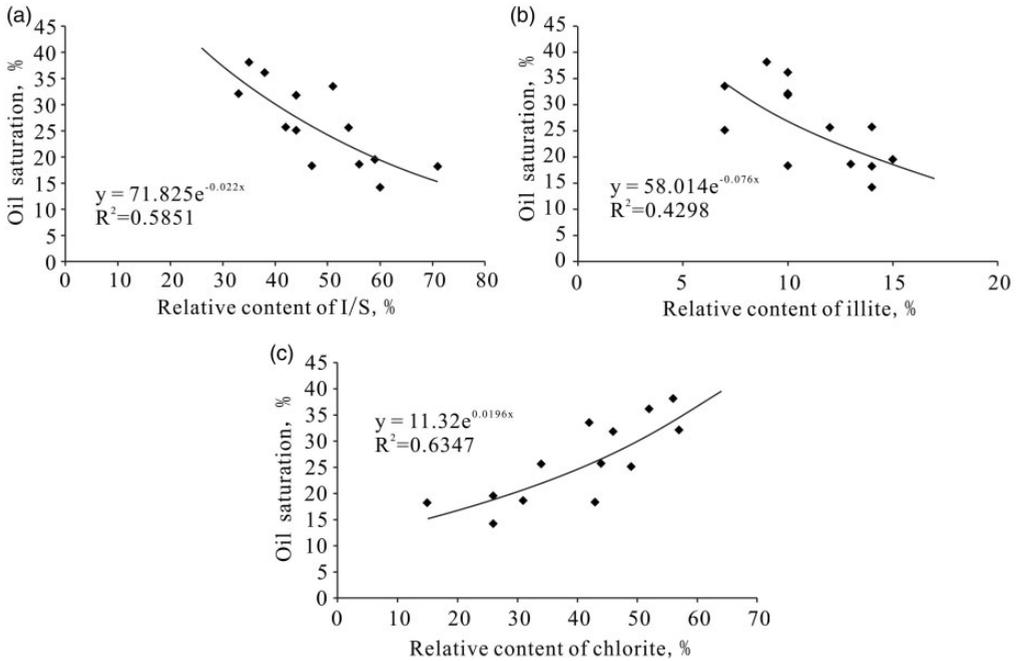
Figure 13. Relationships between the content of I/S, illite, chlorite, and oil saturation in the K_1q_4 tight sandstone reservoirs.

Wardlaw, 1982). Previous studies have proposed some parameters combing porosity and permeability together to reflect the reservoir pore–throat structure and flow characteristics, and applied to tight sandstone reservoir evaluation and favorable exploration target prediction (Amaefule et al., 1993; Lala and El-Sayed, 2015). Among these parameters, reservoir quality index (RQI) and flow zone indicator (FZI) are the mostly used ones. RQI is closely related to pore–throat structures (Amaefule et al., 1993), whereas FZI can reflect the flow characteristics of the reservoir additionally (Lala and El-Sayed, 2015).

FZI is a unique and useful parameter to quantify the flow characteristics of a reservoir and it offers a relationship between petrophysical properties at a small scale and at a large scale, such as between core plugs and wireline log (Lala and El-Sayed, 2015). FZI values are estimated using porosity and permeability, which can be defined as (Lala and El-Sayed, 2015)

$$FZI = RQI/\varphi_r \tag{2}$$

where the $RQI = 0.0314 \times (K/\varphi)^{1/2}$, the pore-to-grain volume ratio $\varphi_r = \varphi/(1-\varphi)$, K is permeability, and φ is porosity.

According to equation (2), FZI not only contains the information of pore–throat structure characteristics, but also reflects other factors, such as diagenetic minerals wettability, related to reservoir flow properties (Lala and El-Sayed, 2015). Therefore, FZI should be a reasonable parameter to predict favorable exploration targets in tight sandstone reservoirs
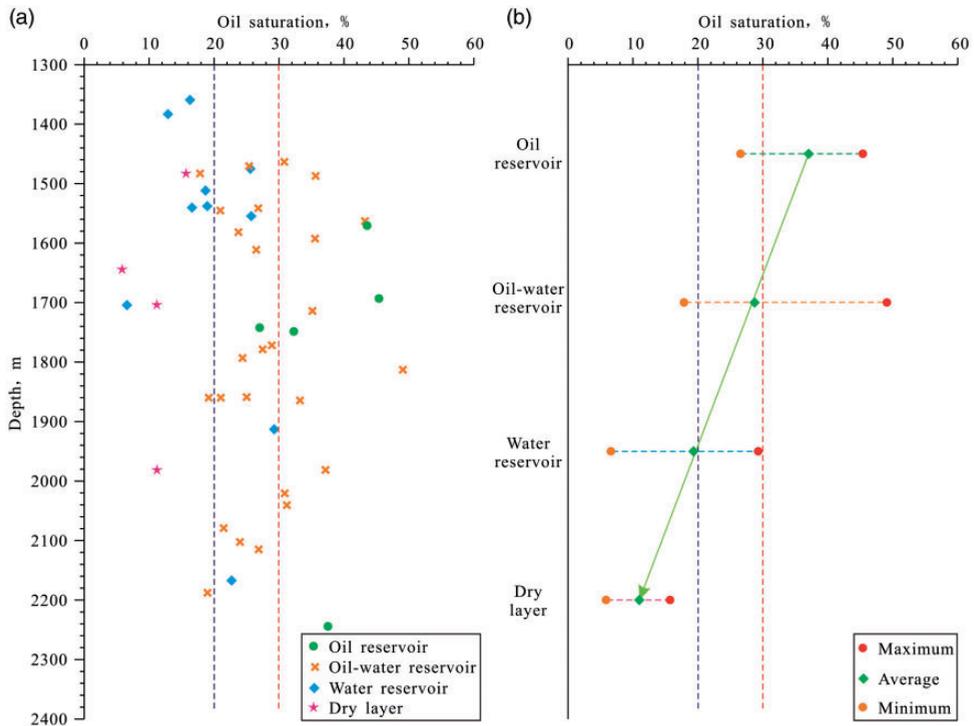
Figure 14. Oil saturation distribution characteristics in oil reservoir, oil–water reservoir, water reservoir, and dry layer according to well test and production test results in the K_1q_4 tight sandstone reservoirs.

because oil emplacement and accumulation in the K_1q_4 tight sandstone reservoirs are mainly controlled by pore–throat and diagenetic minerals as mentioned above.

Relationship between FZI and pore–throat parameters. In the PMI, average pore–throat radius, sorting coefficient of pore–throat, structural coefficient of pore–throat, and median saturation pressure are the typical parameters characterizing pore–throat sizes and distribution, as well as combination patterns of pore–throat radius and volumes. There are positive correlations between FZI and average pore–throat radius, sorting coefficient of pore–throat, structure coefficient of pore–throat (Figure 15(a) to (c)). However, FZI decreases with increasing median saturation pressure of mercury injection (Figure 15(d)). These suggest that FZI values increase when pore–throat structures become progressively better, similar to the relationship observed between oil saturation and pore–throat parameters. Thus, FZI can be used as a synthesis composite parameter to characterize the oil saturation instead of pore–throat parameters.

Relationship between FZI and diagenetic minerals. First, carbonate minerals appear to influence FZI similar to its impact on oil saturation (Figures 12 and 16(a)). When the content of carbonate minerals is lower than about 5%, FZI increases with increasing carbonate mineral content (Figure 16(a)). On the contrary, FZI decreases with increasing carbonate mineral content when the content of carbonate minerals is over 5% (Figure 16(a)). As to the
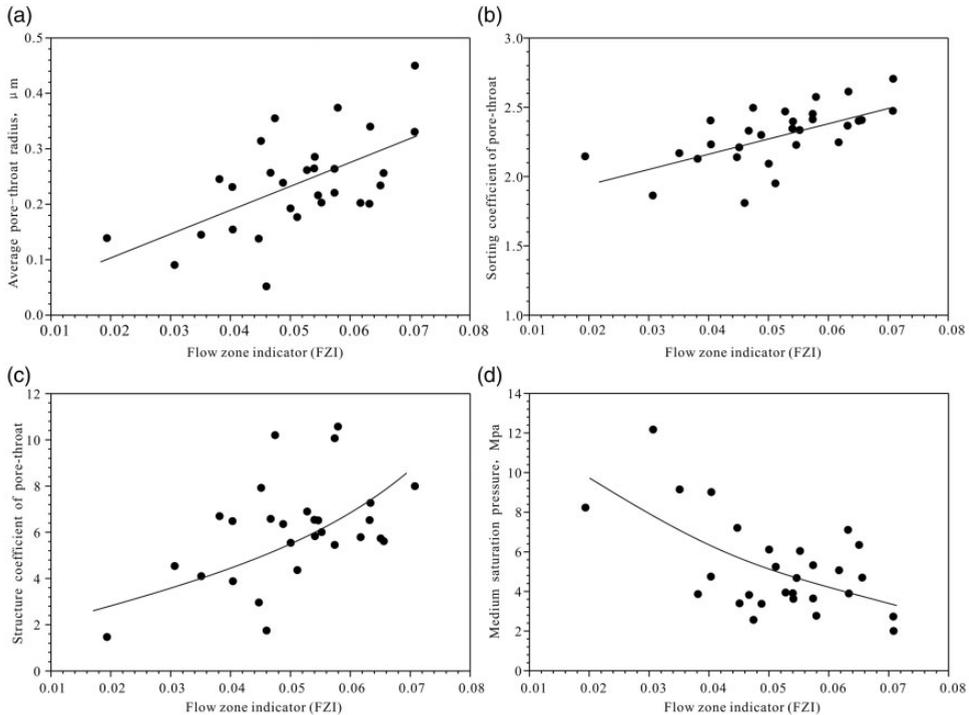
Figure 15. Relationships between FZI and pore–throat parameters in the K_1q_4 sandstone reservoirs.

authigenic clay minerals, the FZI is negatively correlated with the relative content of I/S and illite (Figure 16(b) and (c)), but positively correlated with chlorite content (Figure 16(d)). These correlations match well with the relationship between oil saturation and the relative content of authigenic clay minerals (Figures 13 and 16). Similarly, these relationships support that FZI can be used as a composite parameter to characterize the oil saturation instead of diagenetic minerals content.

Exploration fairway prediction

As a whole, there is a positive relationship between oil saturation and FZI value. Moreover, the distribution of oil saturation shows significant differences among different FZI value ranges (Figure 17(a)). Specifically, oil saturations are lower than 20% when the FZI values are less than 0.03 (Figure 17(a)). In the ranges of FZI values from 0.03 to 0.05, oil saturations vary from 10 to 30% with some being below than 20% (Figure 17(a)). When the FZI values vary from 0.05 to 0.07 oil saturations mainly range from 20 to 40% (Figure 17(a)). When the FZI values are larger than 0.07, oil saturations are mainly higher than 30% (Figure 17(a)). Accordingly, the reservoirs with FZI values larger than 0.05 can be regarded as favorable exploration targets in the K_1q_4 tight sandstones, which are characterized mainly by oil–water reservoirs and oil reservoirs with oil saturations greater than 20% (Figure 17(b)). Reservoirs with FZI values over 0.07 have been shown to have yielded
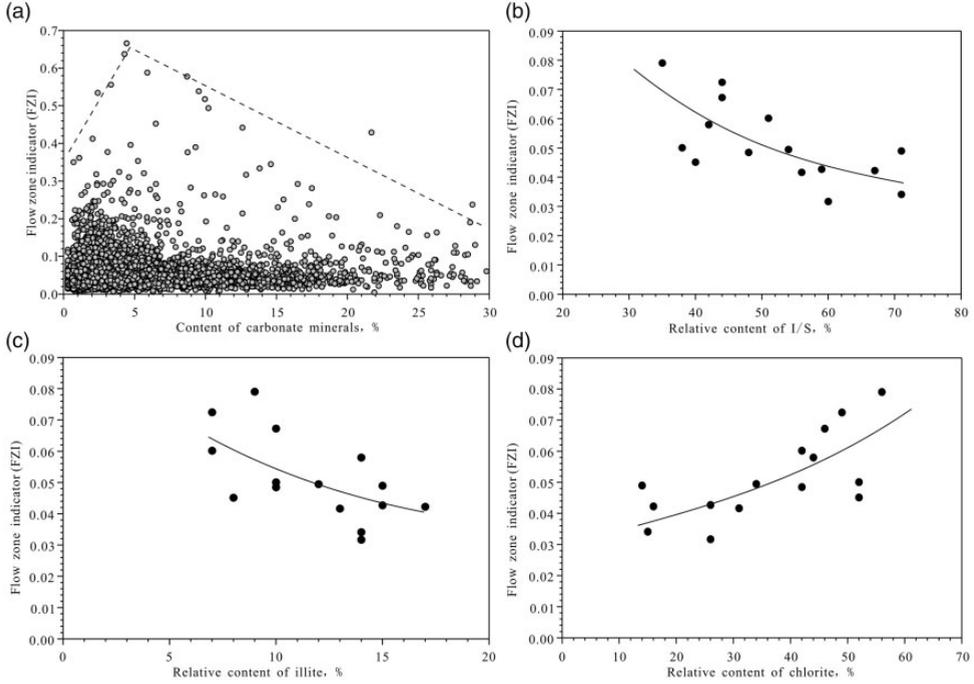
Figure 16. Relationships between content of diagenetic minerals and FZI in the K_1q_4 tight sandstone reservoirs. I/S: illite/smectite.
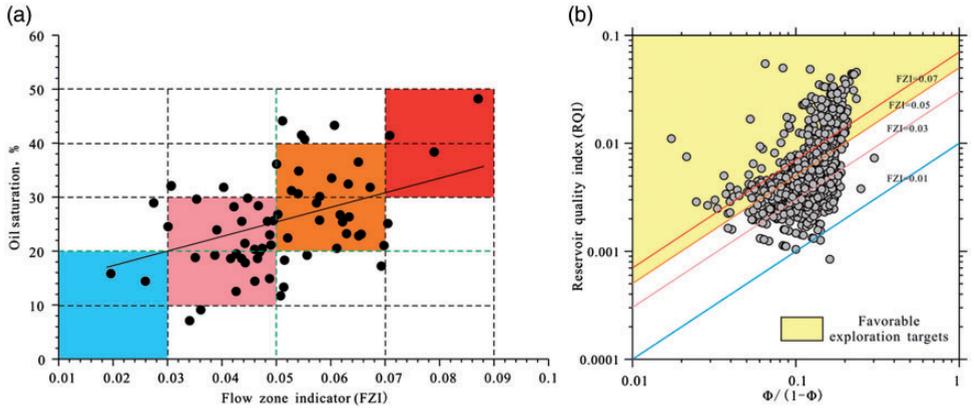

Figure 17. Relationship between FZI and oil saturation (a) and favorable exploration targets determination (b) in the K_1q_4 tight sandstone reservoirs.

relative high oil production, which are characterized mainly by oil reservoirs with oil saturation over 30%.

Based on the studies above, favorable exploration targets were predicted within the first sands group of the K_1q_4 tight sandstone reservoirs as an example. First, porosity and

permeability of the core samples in each cored interval were measured to calculate the FZI value of each core sample. The average FZI values of the first sands group were then calculated for each well. Finally, the average FZI value for the first sands group of the K_1q_4 sandstone reservoirs was contoured. The regions with average FZI values over 0.05 are determined to be the favorable exploration targets in the first sands group of the K_1q_4 tight

Figure 18. Planar isoline of average FZI value and favorable exploration targets prediction for the first sands group of the K_1q_4 sandstone reservoirs. FZI: flow zone indicator.

sandstone reservoirs (Figure 18). The results show that the distribution of the favorable exploration targets accords well with sedimentary facies in the K_1q_4 tight sandstone reservoirs. Overall, the favorable exploration targets were found in the delta plain distributary channel and deltaic front subaqueous distributary channel (Figure 18).

Conclusions

(1) The K_1q_4 tight sandstone reservoirs are characterized by poor reservoir properties and low oil saturations. The reservoir properties measured at laboratory ambient conditions and under in situ conditions are not much different. Reservoirs with similar porosity and permeability sometimes show significantly different oil saturations.

(2) The K_1q_4 tight sandstone reservoirs are dominated mainly by micro-scale pores, and nano-scale pore–throats, forming micro- to nano-scale pore–throat system. Most of the samples are characterized by poor connectivity with effective connected pore–throat network mainly less than 40%.

(3) Oil emplacement mainly occurs via the throats with average radius larger than 0.25 μm under in situ geological conditions in the K_1q_4 tight sandstone reservoirs. Oil saturation increases with increasing average pore and throat radius. Samples with higher oil saturation show wider ranges of pores and throats, but a centered pore–throat radius ratio distribution. The best pore–throat volume ratio for oil emplacement in the K_1q_4 tight sandstone reservoirs is about 2.3–3.0, corresponding to high oil saturation.

(4) Carbonate cements and authigenic chlorite in the K_1q_4 sandstone may help modifying the wettability of some parts of the pores from water-wet to oil-wet, promoting emplacement and accumulation.

(5) The FZI not only contains information of pore–throat structure characteristics, but also can reflect other factors, such as diagenetic minerals wettability, related to reservoir flow properties. Therefore, FZI is a reasonable parameter to predict exploration fairways in the K_1q_4 tight sandstone reservoirs. The reservoirs with FZI values larger than 0.05 can be regarded as favorable exploration targets in the K_1q_4 tight sandstones, which are mainly oil–water reservoirs and oil reservoirs with oil saturation higher than 20%. Generally, the favorable exploration targets distribute in the delta plain distributary channels and deltaic front subaqueous distributary channels.

References

Alotaibi MB, Nasralla RA, Nasr EI, et al. (2011) Wettability studies using low-salinity water in sandstone reservoirs. *SPE Reservoir Evaluation & Engineering* 14(6): 713–725.

Amaefule JO, Altubay MH, Tiab D, et al. (1993) Enhanced reservoir description using core and log data to identify hydraulic flow units and predict permeability in uncored intervals/wells. Society of Petroleum Engineers paper 26436.

Buckley JS (2001) Effective wettability of minerals exposed to crude oil. *Current Opinion in Colloid & Interface Science* 6: 191–196.

Dong T, He S, Wang D, et al. (2014) Hydrocarbon migration and accumulation in the Upper Cretaceous Qingshankou Formation, Changling Sag, southern Songliao Basin: Insights from integrated analyses of fluid inclusion, oil source correlation and basin modelling. *Journal of Asian Earth Sciences* 90: 77–87.

Hillier S (2003) Quantitative analysis of clay and other minerals in sandstones by X-ray powder diffraction (XRPD). In: Worden R and Morad S (eds) *Clay Mineral Cements in Sandstones. International Association of Sedimentologist, Special Publication*. Blackwell Science: Oxford International, pp.213–251.

Jia C (2017) Breakthrough and significance of unconventional oil and gas to classical petroleum geological theory. *Petroleum Exploration and Development* 44(1): 1–11.

Kang Y (2016) Resource potential of tight sand oil and gas and exploration orientation in China. *Natural Gas Industry* 36(10): 10–18.

Lai J, Wang G, Ran Y, et al. (2016) Impact of diagenesis on the reservoir quality of tight oil sandstones: The case of Upper Triassic Yanchang Formation Chang 7 oil layers in Ordos Basin, China. *Journal of Petroleum Science and Engineering* 145: 54–65.

Lala AMS and El-Sayed NAA (2015) Effect of pore framework and radius of pore throats on permeability estimation. *Journal of African Earth Sciences* 110: 64–74.

Law BE (2002) Basin centered gas system. *AAPG Bulletin* 86: 1891–1919.

Li D, Dong C, Lin C, et al. (2013) Control factors on tight sandstone reservoirs below source rocks in the Rangzijing slope zone of southern Songliao Basin, East China. *Petroleum Exploration and Development* 40(6): 692–700.

Moore DM and Reynolds RC (1997) *X-Ray Diffraction and the Identification and Analysis of Clay Minerals*. Oxford: Oxford University Press.

Pang X, Jiang Z, Huang H, et al. (2014) Formation mechanisms, distribution models, and prediction of superimposed, continuous hydrocarbon reservoirs. *Acta Petrolei Sinica* 35(5): 795–828.

Qi Y, Luo X, He Y, et al. (2015) Experimental studies on oil imbibition in mixed-wetting porous medium. *Chinese Journal of Geology* 50(4): 1208–1217.

Shanley KW and Cluff RM (2015) The evolution of pore-scale fluid-saturation in low permeability sandstone reservoirs. *AAPG Bulletin* 99: 1957–1990.

Sun Y, Deng M, Ma S, et al. (2015) Distribution and controlling factors of tight sandstone oil in Fuyu oil layers of Da'an area, Songliao Basin, NE China. *Petroleum Exploration and Development* 42(5): 646–655.

Wang J, Feng L, Steve M, et al. (2015) China's unconventional oil: A review of its resources and outlook for long-term production. *Energy* 82: 31–42.

Wardlaw NC (1982) The effects of geometry, wettability, viscosity and interfacial tension on trapping in single pore-throat pairs. *Journal of Canadian Petroleum Technology* 21: 27.

Wei W, Zhu X, Meng Y, et al. (2016) Porosity model and its application in tight gas sandstone reservoir in the southern part of West Depression, Liaohe Basin, China. *Journal of Petroleum Science and Engineering* 141: 24–37.

Wimmers K and Koehrer B (2014) Integration of sedimentology, petrophysics and rock typing as key to understanding a tight gas reservoir. *Oil Gas European Magazine* 40: 196–200.

Xi K, Cao Y, Haile B, et al. (2016) How does the pore-throat size control the reservoir quality and oiliness of tight sandstones? The case of the Lower Cretaceous Quantou Formation in the southern Songliao Basin, China. *Marine and Petroleum Geology* 76: 1–15.

Xi K, Cao Y, Jahren J, et al. (2015) Diagenesis and reservoir quality of the Lower Cretaceous Quantou Formation tight sandstones in the southern Songliao Basin, China. *Sedimentary Geology* 330: 90–107.

Yang S, Zhang J, Huang W, et al. (2013) "Sweet spot" types of reservoirs and genesis of tight sandstone gas in Kekeya area, Turpan-Hami Basin. *Acta Petrolei Sinica* 34(2): 272–282.

Yu J, Ma J, Lu J, et al. (2015) Application of mercury injection and rate-controlled mercury penetration in quantitative characterization of microscopic pore structure of tight reservoirs: A case study of the Chang7 reservoir in Huachi-Heshui area, the Ordos Basin. *Petroleum Geology & Experiment* 37(60): 789–795.

Zeng J, Yang Z, Feng X, et al. (2014) Study status and key scientific issue of tight reservoir oil and gas accumulation mechanism. *Advance in Earth Sciences* 29(6): 651–661.

Zhang W, Li Y, Xu T, et al. (2009) Long-term variations of CO_2 trapped in different mechanisms in deep saline formations: A case study of the Songliao Basin, China. *International Journal of Greenhouse Gas Control* 3: 161–180.

Zhang X and Zhang L (2013) Quantitative research on effective source rocks of the Denglouku Formation in northern Songliao Basin. *Chinese Journal of Geology* 48(3): 879–890.

Zhao H, Ning Z, Wang Q, et al. (2015) Petrophysical characterization of tight oil reservoirs using pressure-controlled porosimetry combined with rate-controlled porosimetry. *Fuel* 154: 233–242.

Zhou Y, Jia Y, Zhang S, et al. (2016) Controls on reservoir quality of Lower Cretaceous tight sandstones in the Laiyang Sag, Jiaolai Basin, Eastern China: Integrated sedimentologic, diagenetic and microfracturing data. *Marine and Petroleum Geology* 76: 26–50.

Zhou Z, Feng D, Wang H, et al. (2012) Sequence stratigraphy framework of Qing 1 and Qing 2 members in the western slope of southern Songliao Basin and its control effect on reservoir sand bodies. *Lithologic Reservoirs* 24(3): 39–50.

Zhu R, Bai B, Cui J, et al. (2013) Research advances of microstructure in unconventional tight oil and gas reservoirs. *Journal of Palaeogeography* 15(5): 615–623.

Zou C, Jia C, Zhao W, et al. (2005) Accumulation dynamics and distribution of litho stratigraphic reservoirs in South Songliao Basin. *Petroleum Exploration and Development* 32(4): 125–130.

Zou C, Tao S, Yuan X, et al. (2009) Global importance of "continuous" petroleum reservoirs: Accumulation, distribution and evaluation. *Petroleum Exploration and Development* 36(6): 669–682.

Zou C, Zhang G, Yang Z, et al. (2013) Concepts, characteristics, potential and technology of unconventional hydrocarbons: On unconventional petroleum geology. *Petroleum Exploration and Development* 40(4): 413–428.